

Kinetic study and Modeling of heavy Naphtha Catalytic Reforming process in AL-Daura Refinery

Mohammad Fadhil Abid* & Haider Majeed Khothar**

*Chemical Engineering Department-UOT

**Midland Refineries Co. - MoO

Abstract:

In the present work, kinetics and modeling of heavy naphtha catalytic reforming process in AL-Daura refinery-Midland refineries Company were studied. A proposed reaction scheme involving (15 pseudo components) connected together by a network of 30 reactions for components in the C₆-C₈₊ range have been modeled. In the present work, kinetics and modeling of heavy naphtha catalytic reforming process in AL-Daura refinery-Midland refineries Company were studied. A proposed reaction scheme involving (15 pseudo components) connected together by a network of 30 reactions for components in the C₆-C₈₊ range have been modeled. The proposed model has been solved numerically using the 4th order Runge–Kutta approach. Alteration of components and temperature, with time and reactor length was evaluated. Results showed that the rate of formation of aromatics is becoming slower as the reactants proceed to the third reactor. The catalytic reaction rates in the reformer are well represented by the Hougen-Watson Langmur-Hinshelwood (HWLH) type form. The deactivation of catalyst causes the reactor behavior to continue changing over a longer period of time. This clearly seems to pay off in the scenario where coke deposition plays such a major role. It was also found that the rate of coke formation increases with the progress from first to the last bed, so keeping a decreasing inlet temperature profile from first to the last bed would lead to more uniform coke content in each bed. The production rate of reformate has a negative impact on the octane number. Temperature drop across the first reactor (~ 45°C) is larger than the temperature drops across the other two reactors (10-12°C). This could be related to the endothermic reaction rate which is faster in the first reactor. The results show that perfect agreement of temperatures, compositions, and fractions molar flow rate at the exit of the third reactor is obtained between predicted values and industrial values. This confirmed the reliability of the present model.

Keywords: Kinetic study, Naphtha Catalytic reforming, AL-Daura refinery, Modeling

الخلاصة:

البحث الحالي يهدف الى دراسة حركية التفاعلات في مفاعل وحدة تحسين النفثا في مصفى الدورة, اضافة الى اعداد نموذج رياضي للمفاعل, تم اقتراح شبكة للتفاعلات الكيماوية مكونة من ثلاثين تفاعل لخمسة عشر مركب C6-C8+. اوضحت النتائج ان معدل تكوين المواد الاروماتية يتباطأ على امتداد طول المفاعل. كما ان موديل HWLH نجح بشكل جيد في وصف معدل سرعة التفاعل المحفز بالعامل المساعد. و قد لوحظ ان تكون المواد الفحمية على العامل المساعد يتزايد من المفاعل الاول الى المفاعل الثالث ويكون معدل التكون منتظم بانتظام الهبوط بدرجة الحرارة خلال المفاعلات. وقد وجد ان هناك تناسب عكسي بين معدل انتاجية الريفورميت و عدده الاوكتاني. ان الحسابات اظهرت ان الهبوط في درجة الحرارة خلال المفاعل الاول يبلغ اكثر من ثلاثة مرات الهبوط خلال المفاعلين الاخرين.

تم التأكد من موثوقية الموديل الرياضي من خلال مقارنة النتائج العملية للمفاعل مع المعطيات النظرية للموديل الرياضي. كان معدل الانحراف النسبي المئوي لقيم درجة الحرارة, النواتج البارفينية, النفثينية و الاروماتية, والتدفقات المولية ضئيل و هذا يثبت موثوقية الموديل.

Introduction:

The Second World War played a significant role in catalyzing the technological growth of the petroleum industries and catalytic reforming was no exception. Catalytic reforming of naphtha or mixture of naphtha with a certain amount of cracking oil is a process of great interest to the petrochemical industry for the production of aromatic compounds that are raw materials for plastics, elastomers and resins manufacture. Catalytic reforming unit uses naphtha or cracking oil as feedstock to produce rich aromatic compounds and high octane value liquid products through reactions such as aromatization, cyclization, and hydrocracking. At the same time, it produces hydrogen (H₂) and liquefied petroleum gas (LPG) as by-products. The design or simulation of the catalytic reforming reactor is very difficult because of complicated components of catalytic reforming feedstock, higher operating temperature of the system, and the complicated reactions in the reactor [1]. A lot number of articles have appeared in the literature studying the chemistry of reforming reactions. Recently some informative papers published on the modeling of catalytic naphtha reforming would be mentioned. Miguel et al. [2] presented a kinetic and reactor modeling of catalytic reforming of naphtha. They carried out bench-scale isothermal reactor experiments to validate their developed kinetic model. They applied the kinetic and reactor models for the simulation of commercial semi-regenerative

reforming unit, the effect of benzene precursors in the feed in both laboratory and commercial reactors was also simulated. Zaidoon [3] made a one-dimensional steady-state mathematical model of a semi-regenerative naphtha catalytic reforming process including four reactors. The model incorporated a kinetic model involving 24 components, 1 to 11 carbon atoms for paraffins (n and iso) and 6 to 11 carbon atom for naphthenes and aromatics with 71 reactions. The model presented the composition, temperature and pressure distributions along the four reforming reactors. The results showed good agreement between the reformate composition of proposed model with the experimental reformate composition. Raouf et al. [4] carried out experimental and theoretical studies to describe the reaction kinetics in heavy naphtha catalytic reforming process) on tri-metal supported on Al_2O_3 catalysts using catalytic reforming process. They investigated the dehydrogenation, dehydrocyclization, and hydrocracking reactions to characterize the catalysts performance toward higher activity and selectivity to desired products. The concentration, conversion, and temperature profiles have been studied and the results showed a good agreement between experimental and simulation model with a deviation ranging from 4.18% to 19.50%. Zahedi et al. [5] investigated the steady state and dynamic simulation of a fixed bed industrial naphtha reforming reactors. They used a heterogeneous model to investigate the performance of the reactor. The formulated models were validated against measured process data of an existing naphtha reforming plant. The results of simulation in terms of components yields and temperature of the outlet were in good agreement with empirical data. Cochegrue et al. [6] carried out a modeling of refining processes using metal-acid bifunctional catalysts involves an exponentially increasing number of species and reactions, which may rapidly exceed several thousand for complex industrial feedstocks. They reported that due to the large number of elementary steps occurring in bifunctional catalysis, a computer generation of the reaction network according to simple rules offered an elegant solution in such a case. They stated that for several refining processes, reasonable assumptions on the equilibria between species allow to perform an a posteriori relumping of species, thus reducing the network size substantially while retaining a kinetic network between lumps that is strictly equivalent to the detailed network. They illustrated this posteriori relumping approach and successfully applied to the kinetic modeling of catalytic reforming reactions.

The present study aims to analyze the process of catalytic naphtha reforming in AL-Daura refinery and develop, via kinetic mathematical expressions, a valid reformer model that relates the input and output variables of the process and associated coefficients and apply a suitable solution technique to the mathematical statement of the problem.

2-Process Description of Catalytic Naphtha Reforming Unit in Daura Refinery:

The flow diagram of the Daura catalytic naphtha reforming unit modeled in this work is displayed in figure (1). The feedstock to the catalytic reformer are the gasoline boiling range hydrocarbons (80-180°C), collectively known as naphtha, which in the raw crude. These are separated from the other crude hydrocarbons by fractionation in the crude column. The gasoline, or naphtha, obtained directly from crude oil is always of low octane number; therefore the refiner cannot use it as a motor fuel directly, so that the purpose of the catalytic reformer process is to raise the octane number of gasoline to a higher octane number.

The naphtha used as a catalytic reformer feedstock usually contains the mixture of paraffins, naphthenes, and aromatics in the carbon number range (C₅ – C₁₀).

Tables (1, 2) list the operating and geometric variables values associated with the process.

Table (1) Feed and reformat analysis and flows in the given data (Daura Refinery).

Property	Unit	Feed	reformat
Flow	bbl/hr.	412	325
API gravity		55	
PNA analysis			
Paraffins (P)	mol %	47.67	12
Naphthenes (N)	mol %	32.2	1.5
Aromatics (A)	mol %	20.1	47.5

ASTM distillation data			
0%	°C	115	49.5
10%	°C	120.5	86
30%	°C	128	117.5
50%	°C	135.2	135.4
70%	°C	145.8	148.5
90%	°C	165	165.7
100%	°C	185	209.8

Table (2) Reactor bed temperatures, pressure, and catalyst bed weights (Doura Refinery).

Property	Unit	First Bed	Second Bed	Third Bed
Pressure Drop	bar	0.23	0.22	0.21
Inlet Temperature	°C	486	486	485
Outlet Temperature	°C	454	467	473
Catalyst weight	kg	5000	12000	18000

As shown in figure (1), total reactor charge is heated, at first by exchange with effluent from the last reactor, and is finally brought up to the first reactor inlet temperature in the first charge heater also called as first inter heater. The reactor effluent-to-feed exchanger recovers the heat from the reactor effluent and provides it to the reactor feed. Thus it is one key to energy conservation in a catalytic reformer. The reactor effluent which may as high as (470 to 475°C) must be cooled to (250°C) for flash separation of hydrogen from reformate.

After passing through the reactor effluent-to-feed exchanger and the charge heater, the total reactor charge is (100% vapor), is up to reaction temperature, and is ready to contact the reforming catalyst. The most commonly used catalyst type is platinum on alumina support. The flow scheme figure (1) shows three reactors in series.

The reactor feed was raised to the proper temperature for the reforming reactions to occur when the charge contacts the catalyst. As shown in figure (1), total reactor charge is heated, at first by exchange with effluent from the last reactor, and is finally brought up to the first reactor inlet temperature in the first charge heater also called as first inter heater. (Effluent is total vapor flowing out of the last reactor.) The reactor effluent-to-feed exchanger recovers the heat from the reactor effluent and provides it to the reactor feed.

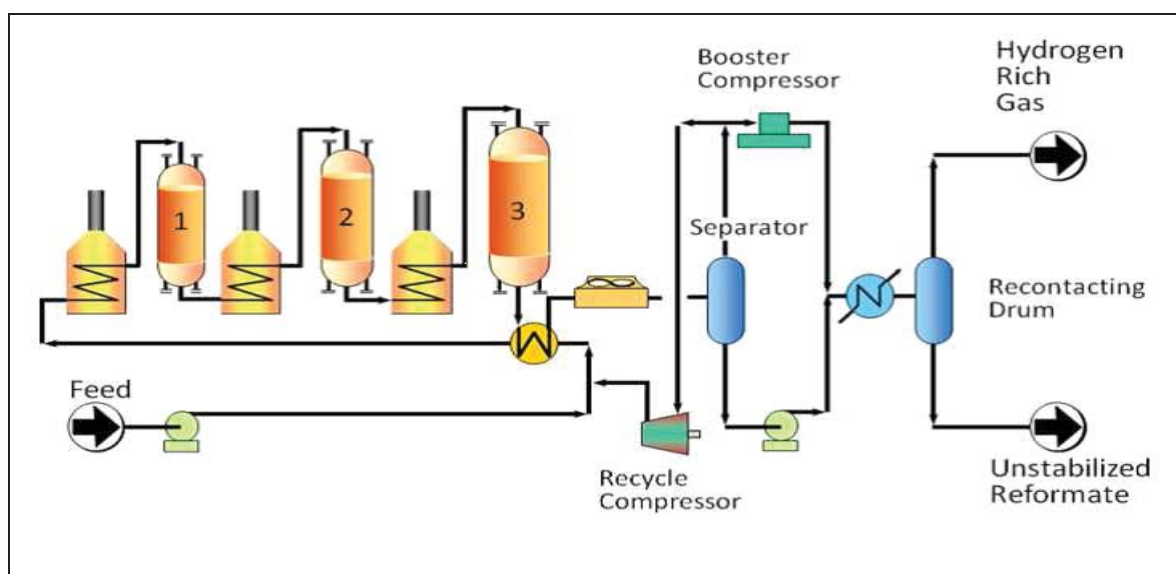


Fig. (1) Process flow scheme of the catalytic naphtha reformer in Al-Doura Refinery.

3-Modeling of a Catalytic Naphtha Reformer:

A kinetic model defines the rates of various reactions and the associated heat and material balance using a system of equations. Developing a kinetic model from basic reaction kinetics and fundamental engineering relationships is a major investment in engineering resources. In the present kinetic model (C_1 to C_5) hydrocarbons are specified as light paraffins and the (C_6 to C_{8+}) naphtha cuts are characterized as isoparaffins, normal paraffins, naphthenes and aromatics. Mole fractions of naphtha cuts with more than nine carbon number are very low and therefore are lumped together.

3.1 Assumptions of the kinetic model

The characteristics and the assumptions made in the kinetic model in this work are listed below:

a-The selected reversible reaction network was proposed by (Arani et al, 2009) ^[7] is shown in figure (2).

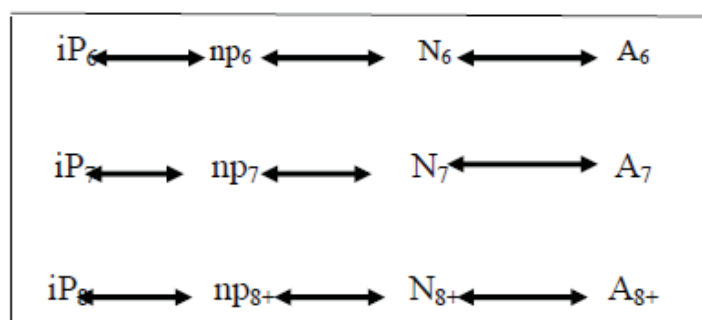


Fig.(2)Reversible reaction networks [7].

b-The paraffin in each carbon number group are divided into three individual pseudo-components; straight chain, single branched and multi-branched.

c-Five-carbon ring naphthenes or alkylcyclopentanes in each carbon number group are lumped together.

d-Under the reaction conditions, aromatics and naphthenes hydrocracking to lower carbon number paraffin is almost negligible.

e-All the rate coefficients obey the well-known Arrhenius' law, thus making them exponentially dependent on the temperature.

f- Van't Hoff equation [9] would be used to evaluate equilibrium constraints of reversible reactions.

g-It is assumed that the reaction rate equations obtained by analyzing experimental conversions for (C₆-C₈) hydrocarbons suggested by [8] are applicable in the present work.

Table (3) Reaction rate equations obtained by analyzing experimental conversions for (C₆-C₈) hydrocarbons [8].

Type of reaction	Reaction Rate Expression
Isomerization of paraffins	$r = A_0 e^{-E/RT} \frac{(P_A - P_B / K_{A,B})}{I}$
Hydrocracking of single branched and Multiple branched paraffins	$r = A_0 e^{-E/RT} \frac{(P_A - P_H)}{I}$
Ring closure of n-paraffins	$r = A_0 e^{-E/RT} \frac{(P_A - P_B - P_H) K_{A,B}}{I}$
Ring expansion of alkylcyclopentanes To Alkylcyclohexanes	$r = A_0 e^{-E/RT} \frac{(P_A - P_B / K_{A,B})}{I}$
Dehydrogenation of methyl cyclo hexane	$r = A_0 e^{-E/RT} \frac{(P_A - P_B - P_H^3 / K_{A,B})}{(P_H \theta)}$

Where:

I : Adsorption term for the(acid function)

$$I = (P_H + K_{C6}P_{C6} + K_{P7}P_{P7} + K_{N7}P_{N7} + K_{TOL}P_{TOL})$$

θ : Adsorption term for the Metal function

$$\theta = 1 + K_{MCH}P_{MCH} + K_{MCH} (P_{MCH}/P_H^2)$$

3.2 Selection of deactivation model

The empirical Voorhies correlation [10] for coking in the catalytic cracking of gasoil,

$$C_c = At^n \text{ with } 0.5 < n < 1 \dots\dots\dots (1)$$

Where (t) is the process on-stream time. This correlation has been widely accepted and generalized beyond the scope of the original contribution [11]. Obviously coke is formed from the reaction mixture itself therefore the rate of coking must depend on the composition of the reaction mixture, the temperature, and the catalyst activity and not only on the process on stream time. Several of the overall reactions in catalytic reforming require formation of olefinic

intermediates in their elementary reaction sequence. Ultimately, these olefinic intermediates lead to coke formation and subsequent catalyst deactivation. Catalyst deactivation is primarily caused by the blockage of active sites due to the coke formed from these olefinic intermediates. For example, in the ring isomerization reaction, methycyclopentane forms a methylcyclopentene intermediate in its reaction sequence to cyclohexane. The intermediate can be further dehydrogenated to form methylcyclopentadiene, a coke precursor. A methodology of characterizing the deactivation of a catalyst by coke deposition due to olefins formation and cyclization was developed by [12] and [8]. This approach is utilized in the present work and described as follow: Coke deposition causes a deactivation of the catalyst which can be described by introducing a deactivation function, (η) that multiplies the reaction rates at zero coke content [16].

$$r_i = r_i^0 \eta_i \quad 0 \leq \eta_i \leq 1 \dots\dots\dots(2)$$

The same approach can be taken to describe the decrease of coking rate itself

$$r_{ck} = r_{ck}^0 \eta_{ck} \quad 0 \leq \eta_{ck} \leq 1 \dots\dots\dots(3)$$

where,

$$dC_c/dt = r_{ck} \dots\dots\dots(4)$$

The coke content differential equation is integrated in time to obtain the coke profiles in time. The deactivation function was related to the coke content on the catalyst, i.e., $\eta = f(C_c)$. Amongst the several empirical expression tested for the deactivation function, an exponentially decreasing function, $\eta = (e^{-\alpha C_c})$, led to the best global regression of the isomerization data [12]. Various reaction paths were considered by [8]. They proposed that, the three significant contributions to coke formation which were selected to describe the rates of coke formation reactions are shown schematically in Table (4).

Table (4) Coking reaction scheme and rate equations, for (C₇) hydrocarbons [8].

Coking reaction	Rate equation
Toluene + Alkylcyclopentane \rightarrow Coke	$K_{C1}P_{TOL} * P_{N7} / P_H^2$
Toluene + Alkylcyclohexane \rightarrow Coke	$K_{C2}P_{TOL} * P_{MCH} / P_H^2$
n-Heptane \rightarrow Coke	$K_{C3}P_aP_7 / P_H$

3.3 Modeling of the fixed-bed reactors

The following assumptions would be utilized to formulate the modeling of reactor:

- The flow is assumed to be well distributed on the catalyst by good designed inlet distributor.
- The reaction rate expressions followed the Hougen-Watson Langmuir-Hinshelwood (HWLH) type form which takes into account the heterogeneous nature of the reactions, while the uncertainty associated with internal and external diffusion effects is lumped into the rate parameters [13], [14].
- Axial dispersion of mass is not significant, since the tube length to pellet diameter ratio is greater than 50, while that of heat is also negligible if the same ratio is above 300 [15].
- In the absence of the dispersion effects, it is possible to model the reactor as a pure "plug-flow" type reactor, in which the fluid is taken to move as a plug through the reactor.

3.4 Fixed-bed reactor modeling equations

The reactor model consists of the following differential equations for mole and energy balance, which are integrated through the reactor system. (Ergun's equation) for calculating the pressure drop is also included in the differential format, these equations are found elsewhere [16].

$$\frac{dF}{dW} = \sum_{j=1}^{n_r} \gamma_{i,j} r_j \quad i=1,2,\dots,n_c \quad (5)$$

$$\frac{dT}{dW} = \frac{\sum_{j=1}^{n_r} r_j (-\Delta H_{R_j})}{\sum_{i=1}^{n_c} F_i C_{P_i}} \quad (6)$$

$$\frac{dP}{dW} = -\frac{G}{\rho d_p \phi^3} \left(\frac{150(1-\phi)\mu}{d_p} + 1.75G \right) \frac{1}{A_c \rho_c} \quad (7)$$

3.5 Model solution

The model of the catalytic naphtha reformer described in the earlier sections contains a number of parameters whose initial values were estimated from the literature data and data obtained from process log-sheet of reforming unit in AL-Doura refinery, and sometimes under varied operating conditions. The data provided contained information regarding the following operating variables. Equations 5, 6 and 7 are first order nonlinear differential equations which could be solved simultaneously by finite difference approach using Runge-Kutta method [16, 22].

4. Calculation of the physical properties.

Physical properties were estimated using the empirical correlation developed by (Riazi and Daubert, 1980) [17]

$$\Theta = \alpha A^\beta B^\delta \quad \dots \quad (8)$$

Where (Θ) is the physical property to be predicted. (A and B) can be any two parameters capable of characterizing the molecular forces. The values of correlation constants (α, β, δ) required to evaluate various properties are given in the Table (5), as given by [17]. Thus average TBP and specific gravity of each volume fraction are used to compute its physical and thermodynamic properties. The properties for each cut fraction are estimated,

based on the experimental data by using the minimization technique of the least squares regression method, and tabulated in Table (6)

Table (5) Correlation constants for Equation (8).

Property	Unit	α	β	δ
Molecular Weight	g/mole	5.384×10^{-3}	3.60	-1.03
Molar Volume	cm ³ /mole	3.151×10^{-4}	3.23	-1.668
Critical Pressure	bar	5.42×10^7	-3.33	3.25
Critical Temperature	K	20.2	0.66	0.46
Critical Volume	cm ³ /mole	1.97×10^{-4}	3.25	-1.779
Heat of Vaporization	J/mole	40.56	2.14	0.03

Table (6) Calculated properties for TBP fractions based on the empirical correlation of [17].

True Boiling Point Cut Fraction, %	Molecular Weight	Molar volume, cm ³ /mol	Critical Pressure, bar	Critical Temp, °C	Critical volume, cm ³ /mol	Heat of vaporization, J/mol
0-10	98	133.2	33.5	280	379.6	32062
10-30	107	142.3	31.5	300	418.1	33666
30-50	114.8	150.4	29.5	318	446.0	35179
50-70	123.7	159.6	28.0	331	475.7	36610
70-90	132	170.5	26.3	349	515.5	38455
90-100	146.7	185.7	24.2	375	569.2	40948

5. Parameters estimation

The most critical step performed in the model effort was to estimate the unknown parameters on the basis of provided data. The following different types of parameters had to be determined in this work.

*Parameters used in rate expressions of reforming reactions are as follows: Pre-exponential factors used in evaluating rate constants, activation energies of reforming reactions rate expressions, adsorption equilibrium constants accounting for adsorption of chemical species on the catalyst surface.

* Parameters used for catalyst deactivation: Pre-exponential factors and activation energies of coke formation reactions, deactivation constant, the task involved was to evaluate these parameters such that for a given set of input variables the model predicted the output that matched with the output obtained from the industrial data. Since the number of reactions was (15), the number of pre-exponential factors and the activation energies themselves amounted to (30). This would give an idea about the dimensionality of the problem involved. The input variables to the system are: molar feed rate of each chemical species in feed naphtha, reactor bed inlet temperatures, reactor pressure, and recycle ratio. The adjustable parameters in the model used for fitting the data were the pre-exponential factors and activation energies, which basically decide the rate constants of reforming reactions, and the adsorption equilibrium constants accounting for adsorption of chemical species present in the reaction mixture. The kinetic scheme representing the reactions taking place consists of (15) reactions in (C₆-C₈+) range. Since each reaction rate is characterized by a unique set of activation energy and pre-exponential factor, this implies that rate parameters by themselves account for (30) constants to be evaluated. However, the number of unknown parameters can be reduced by judicious selection of certain parameters to be estimated or pre-decided based on published literature data and studies of reforming reactions carried out in the past. A standard least squares approach was adopted to solve the regression problem [18].

The minimization technique used to evaluate the model parameters is presented in equation (9),

$$\phi = \sum_{i=1}^n w_i (f_i - y_i)^2 \dots\dots\dots(9)$$

Where, (y_i) are the known values (molar flow rates at the exit of last bed calculated from the given data), and (f_i) are known function values (molar flow rates at the exit of last bed predicted by the model), then the algorithm seeks to find a set of (x_i) that will minimize a user defined function,

Deactivation kinetics is simulated by means of coke formation on catalyst surface. Data fitting for determining the kinetic rate parameters of coking reactions would involve collecting the data sets at periodic time intervals over a sufficient run length of the catalyst. Due to non-availability of data at this time, the only option was to use the values given in the literature directly [19] and [8]. The deactivation parameter, (α) was employed as the adjustable parameter, (α) was adjusted so that the product properties predicted by running the model over about one month period of continuous operation would approximately match with that reported in the given data after within the same period. (Trimpont et al., 1988)^[8] reported that analysis of the data collected over a sufficient run length of the catalyst in a heavy naphtha reforming plant, operated at pressure=3 bar and inlet temperature = 763 K , for $\alpha=14.95$, the catalyst deactivation function η vs. coke content is presented in Table (7). These values were inserted into eq.2 to account for coking rate in the present work.

Table (7) catalyst deactivation function η vs. coke content [8].

no.	deactivation function (η)	coke content (C_c), wt%	no.	deactivation function (η)	coke content (C_c)
1	0.9	1	6	0.2	7
2	0.7	3	7	0.18	8
3	0.5	3.6	8	0.16	9
4	0.3	5			
5	0.25	6			

6. Results and Discussion

6.1-Temperature profile along the length of the catalyst bed

Figure (3) displays the temperature profile in each catalyst bed. All the three reactors are operated at about equal inlet temperatures of (486 °C) and the recycle ratio is maintained at (8.73). In fact, this is the base of case operating conditions at AL-Daura refinery. As can be seen, a distinct drop in temperature is observed at the inlet of the first bed. This may be attributed to the immediate occurrence of naphthene dehydrogenation reactions which are considered kinetically as the fastest and most endothermic of all the reactions due to their lower activation energies comparing with other reactions. Table (8) lists the activation energies of some reactions computed by least squares regression.

Table (8) Activation energies of some reactions computed by least squares regression.

no.	reaction	activation energy, kcal/mol
1	$P \xrightarrow{\quad} N + H_2$	35.85
2	$N + H_2 \xrightarrow{\quad} P$	25.96
3	$N \xrightarrow{\quad} A + 3H_2$	16.55
4	$P + H_2 \xrightarrow{\quad} 2G$	26.84

This drop in temperature instantly cools the reaction mixture and decelerates the rates of all the reactions. Consequently, the temperature profile shifted down in the latter part of the bed. The total temperature drop in the first bed is about (32°C) and the reaction mixture needs to be reheated before any further reactions can be carried out. After passing through the first inter-heater, the reaction mixture enters the second catalyst bed. Most of the remaining naphthenes are dehydrogenated in the second bed and this leads to a net temperature drop of about (16°C). The reaction mixture is reheated again to push the reaction rates of paraffins to naphthenes which are the most desirable reactions from reforming point of view, as far as possible and passed through the third bed. These reactions are the most difficult to carry out and slowest to proceed followed by dehydrogenation naphthenes to aromatics, creates an endothermic temperature drop in the third bed.

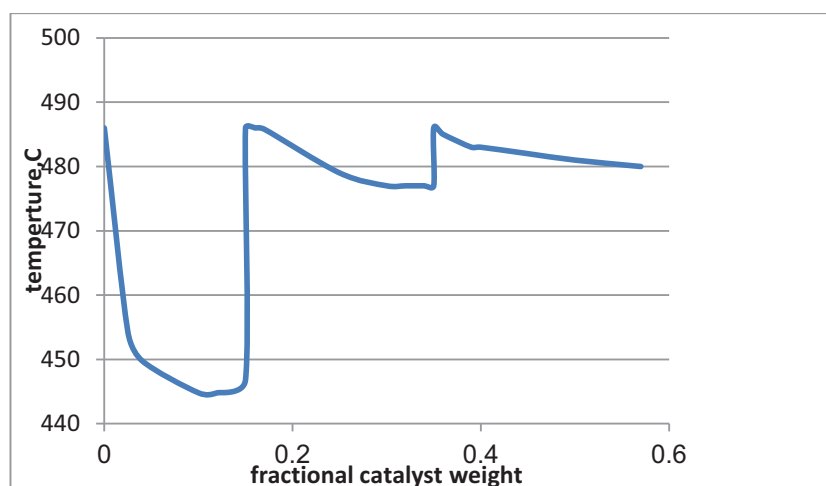


Fig. (3) Temperature profile across the catalyst beds.

However, the rate of temperature drop is relaxed by increasing rates of hydrocracking reactions, which are exothermic in nature. The temperature drops in third reactor are about (10 to 12°C). Our results are in agreement with the findings of [3,5]. Table (9) lists the actual and model values of the output temperature of reactors with their corresponding average relative errors.

Table (9) Output temperature of reactors (°C).

Item	actual	model	Mean absolute percentage Error, %
T1 (°C)	445	447	0.45
T2 (°C)	476	477	0.48
T3 (°C)	479	478	0.21

6.2 Composition profile along the length of the catalyst bed

Figure (4) depicts the composition profiles of major components (i.e., paraffins, naphthenes, and aromatics) as well as lighter cracked gases. As pointed out earlier, the most significant reaction in the first bed is the dehydrogenation of naphthenes. This is realized by sharp decrease in naphthene concentration through the catalyst bed and consequent increase of the aromatics formed. After the product is reheated to (486 °C) for second reactor inlet, the remaining naphthenes, particularly, five-carbon ring naphthenes are isomerized to six-membered rings, which are subsequently dehydrogenated to aromatics. As the five-carbon ring naphthenes are reacted and proceed, the (C₆+) paraffins concentration, starts to fall in the second bed. Isomerization of paraffins also continues to proceed in the first and the second bed. By the end of second bed paraffin isomers are at equilibrium. In third bed, the ring closure reactions of paraffins are carried out, which are also accompanied by hydrocracking reactions of paraffins. Hydrocracking reactions proceed at very similar rates to ring closure. Consequently, concentration of paraffins keeps dropping. Although figure (4) shows a slight decline in aromatics concentration due to ring closure reactions, there is an increase in the net amount of aromatics. This may be attributed to the effect of much higher cracked products presence in the reactor. The findings of [20,23] were in agreement with our results. Table (10) lists product mole flow rate data of (C5-C8+) compared with model predictions.

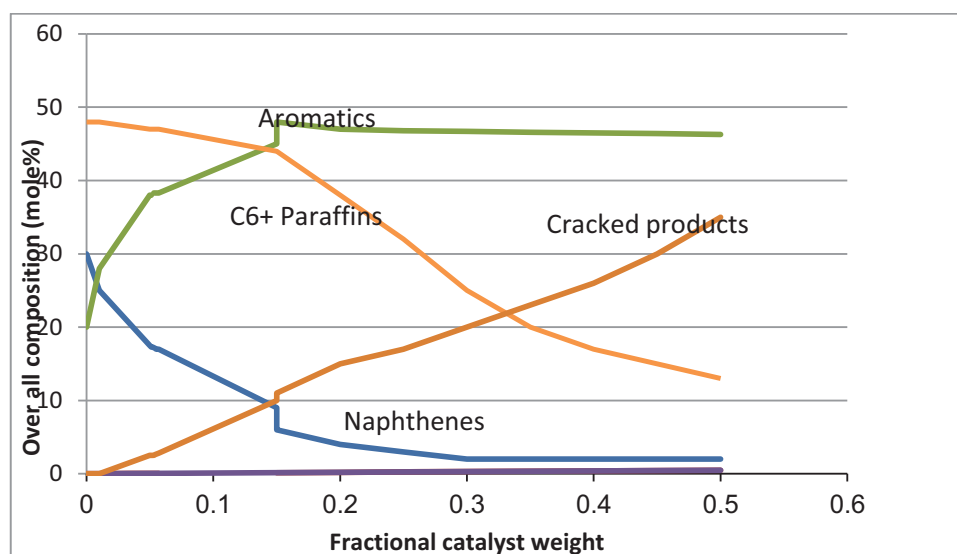


Fig.(4) Profile of main component types through reactor system.

Table (10) product (C5-C8+) mole flow data compared with model predictions*.

Item	Actual, mol/h	Model, mol/h	Mean absolute percentage error, %
C5 fraction	33.22	32.71	1.55
C6 fraction	5.85	5.31	1.01
C7 fraction	21.45	20.17	0.634
C8 fraction	41.07	42.22	0.272
C9 fraction	18.86	19.33	0.249

* Cracked light gases are excluded from table (8).

6.3- Profile of octane number and reformat yield

Figure (5) illustrates the behavior of the most important product property, i.e., research octane number (RON) of reformat, and the volumetric production rate of reformat along the reactor bed. As can be seen from figure (5), there is an inverse relationship between the RON of reformat and its production yield. The octane number increase is related to aromatics formation in the reactors. The feed octane number of 55 rises up to 74 in the first two beds, mainly on

account of naphthenes dehydrogenating to aromatics. However, one more catalyst bed is needed to raise RON up to the desired range of around (90 to 95) a more catalyst bed is needed. This enhancement of RON is conducted by two types of reactions, the ring closure reaction of paraffins and the hydrocracking reactions, which perform the job of removing low octane number paraffins from reformates. In fact, it is supposed that with deactivation of the catalyst, when the reactor severity is increased (i.e., higher temperature and/or pressure), more of the boost in octane number comes from hydrocracking than ring closure. Of course this happens at a cost of loss of the product reformat yield. In general, all reforming reactions involve loss of volume and hence it is typical to end up with a reformat yield of around (70 to 80%).

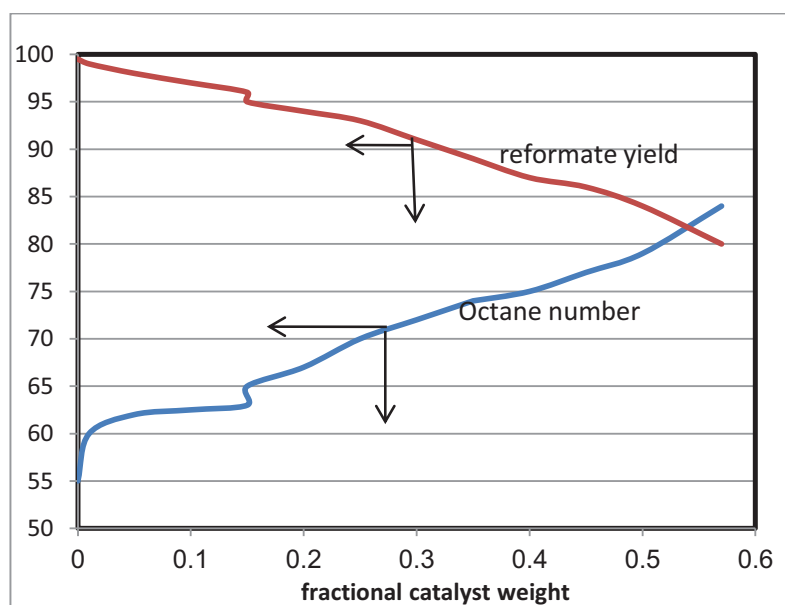
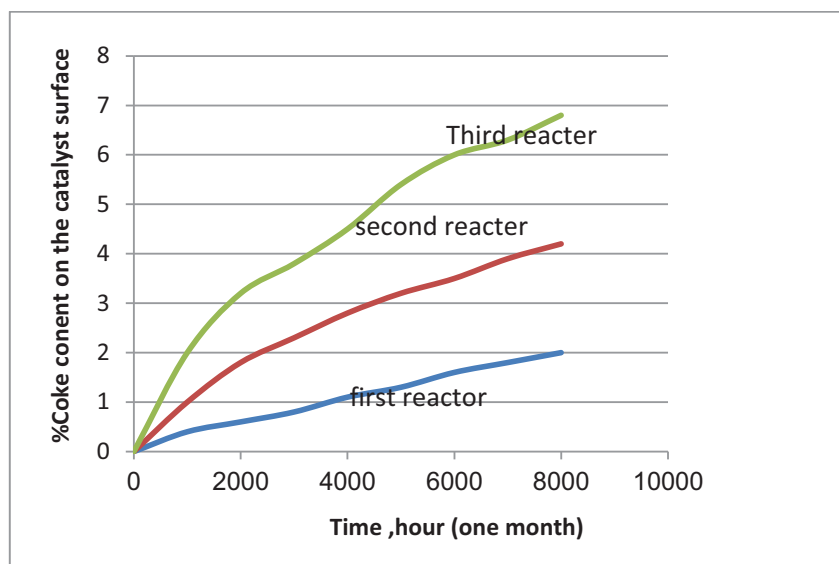


Fig.(5) Volumetric reformat yield and research octane number along the reactor system.

Our results observed and described in Figures (4 - 5) agree quite well with that seen in the industrial practice [20, 21].

6.4-Profile of Coke Content

Figure (6) shows the average coke content on the surface of the catalyst in each bed. Coke content is calculated as weight of coke deposited per unit weight of the catalyst and is plotted on a percentage basis. Average coke content increases from first to the last bed. However, at higher temperatures, rates of hydrocracking reactions increase sharply, which are undesirable reactions from reforming point of view. Although, it has slightly higher activation energy than other reactions, it accelerates coke formation causing a rapid catalyst deactivation. It is worth to notice that that coke formation reactions themselves could be get suppressed due to deactivation of the catalyst. Predicted results of the present model are well agreed with the findings of [4,12].



**Fig. (6) Accumulation of average coke content in each bed over the life of catalyst.
(At constant reactor operating conditions).**

6.5-Variation of Volumetric yield and octane number over the life of catalyst

In figure (7) variation of octane number and reformate yield over the catalyst run length is plotted. As can be seen, octane number and reformate yield always vary in opposite directions. This is quite logical because of the fact that major reforming reactions, such as dehydrogenation of naphthenes and ring closure of paraffins are accompanied by a loss in volume. As expected,

the octane number keeps declining with time since the reforming reactions are adversely affected due to deficiency of catalyst activity by coke formation. The reformate yield increases at the same time, because the major source of the loss of reformate yield, i.e., hydrocracking takes place to a lower extent. In actual operation, reactor inlet temperatures are usually raised to adjust octane. So these plots, which are prepared at a constant inlet temperature, may not resemble the operating scenario. Nonetheless, they are useful from the perspective of purely studying the effect of coking on reformate quality and yield, and for model verification.

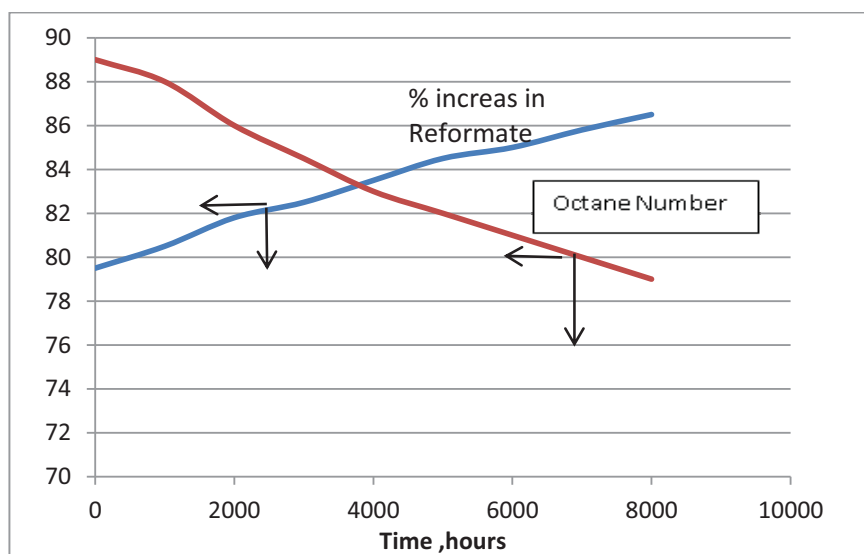


Fig.(7) Variation of Volumetric yield and octane number over the life of catalyst (under constant reactor operating conditions)

7. Model validation

A comparison of the predicted values shown in figures (3, 4) with the experimental data of the reforming unit, listed in Tables (1, 9, & 10) is presented in Table (11). The results show that perfect agreement of temperatures, compositions, and fractions molar flow rate at the exit of the third reactor is obtained between predicted values and reported values which confirmed the reliability of the present model.

Table (11) Comparison of predicted values and plant data for temperature, composition and molar flow rates at effluent of the third reactor.

Output temperature from reactors, °C	Plant data, °C	Model, °C	Mean absolute percentage error, %
T1	445	447	0.45
T2	476	477	0.48
T3	479	478	0.21
Stream Composition at output from third reformer, mol%	Plant data, mol%	Model, mol%	Mean absolute percentage error, %
Aromatic	47.5	50.5	6.0
Naphthen	1.5	1.3	13.0
Paraffins (C ₆₊)	12	10.8	1.0
Molar flow rate of fractions at output from third reformer, mol/h	Plant Data. mol/h	Model, mol/h	Mean absolute percentage error, %
C5 fraction	33.22	32.71	1.55
C6 fraction	5.85	5.31	1.01
C7 fraction	21.45	20.17	0.634
C8 fraction	41.07	42.22	0.272
C9 fraction	18.86	19.33	0.249

7. Conclusions

An industrial naphtha reactor was modeled by heterogeneous model. The proposed model has been solved numerically using the 4th order Runge–Kutta approach. Alteration of components and temperature, with time and reactor length was evaluated. Some conclusions could be withdrawn from the present study:

- 1- The rate of formation of aromatics is becoming slower as the reactants proceed to the third reactor. This may be attributed to a continuous decrease in the concentration of reactants (i.e., paraffins and naphthenes).
- 2- The catalytic reaction rates in the reformer are well represented by the Hougen-Watson Langmur-Hinshelwood (HWLH) type form.
- 3-The deactivation of catalyst causes the reactor behavior to continue changing over a longer period of time. This clearly seems to pay off in the scenario where coke deposition plays such a major role.
- 4- The rate of coke formation increases with the progress from first to the last bed, so keeping a decreasing inlet temperature profile from first to the last bed would lead to more uniform coke content in each bed
- 5- The production rate of reformate has a negative impact on the octane number.
- 6- Temperature drop across the first reactor is larger than the temperature drops across the other two reactors. This could be related to the endothermic reaction rate which is faster in the first reactor due to higher reactant concentration.
- 7- The reforming model contains a rich set of model features with experimental observations suggests that the model is a good platform for additional process specific refinement.

Nomenclature

A	Aromatics
A_0	Pre – exponential factor.
A_c	Cross section of flow in reactor (A_c), m^2
B	Product
C	Carbon Atoms
C_c	Coke content
C_{p_i}	Heat capacity of lump i (kJ/kg. K)
D_p	Diameter of catalyst particle (m)
E	Activation energy. (kJ/mole)
f	Hydrocarbon molar composition
F_i	Molar flow rate of species i (kmol/h)
H_2	Hydrogen
ΔH	Enthalpy of formation. (kJ/mole)
ΔH_{R_i}	Heat of reaction for component j, (kJ/mole)
iP	Iso Paraffins
G	Superficial mass velocity of gases ($kg/m^2.h$)
K	Equilibrium constant
N	Naphthenes
n_c	Number of components lumps.
nN	Normal Naphthenes
nP	Normal Paraffins
MW	Molecular weight, (kg / kmol)
MCH	Methyl Cyclohexan
R	Constant of gases,(kJ / kmol..K)
r_i	Rate of reaction i (kmol/kgcat.h)
r_i^0	Reaction rates at zero coke content.(kmol/kgcat.h)
P	Paraffins

P_i	Partial pressure of component i (kPa).
w	Weight of the catalyst (kg)
$y_{i,j}$	Molar fraction.
<u>Greek Letters</u>	
η	Deactivation function
ϕ	Bed void fraction.
μ	Viscosity of gas. (Pa. s)
ρ	Density of gas mixture ,(kg/m ³)
ρ_c	Density of solid catalyst ,(kg/m ³)
$\gamma_{i,j}$	Stoichiometric coefficient
α	Deactivation parameter.

References

- 1- Liang K., Guo H., Pan S., A study on naphtha catalytic reforming reactor simulation and analysis, Journal of Zhejiang University SCIENCE, 6B(6):590-596. (2005).
- 2- Miguel A. Rodríguez, Jorge Ancheyta, Detailed description of kinetic and reactor modeling for naphtha catalytic reforming, Fuel Journal, Volume 90, Issue 12, Pages 3492–3508. (2011).
- 3- Zaidoon M. S., Catalytic Reforming of Heavy Naphtha, Analysis and Simulation, Diyala Journal of Engineering Sciences, Vol. 04, No. 02 , pp. 86-104. (2011).
- 4- Raouf R.S., Sukkar A.K., Hamied S.R., Heavy Naphtha Reforming Reactions with Tri-metallic Catalysts, Experimental and Analytical Investigation, Eng.& Tech. Journal, Vol. 29, No.10, pp.1917-1935 (2011).
- 5- Zahedi G., M. Tarin, M. Biglari, Dynamic Modeling and Simulation of Industrial Naphta Reforming Reactor, World Academy of Science, Engineering and Technology, 67, pp.911-916 (2012).
- 6- Cochegrue H., P. Gauthier, J.J. Verstraete, K. Surla, D. Guillaume, P. Galtier and J. Barbier, Reduction of Single Event Kinetic Models by Rigorous Relumping: Application to Catalytic Reforming, Oil & Gas Science and Technology – Rev. IFP Energies nouvelles, Vol. 66, No. 3, pp. 367-397 (2011).
- 7- Arani .H.M., Shirvani 2 M.. Safdarian K. And .Dorostkar, Lumping procedure for a Kinetic model of catalytic naphtha reforming, Braze.J.Chem.Eng, Vol.26, No.4 Oct./Dec.(2009).
- 8- Van Trimpont, P. A., Marin, G. B., Froment, G. F., Reforming of C7 Hydrocarbons on a Sulfided Commercial Pt/Al₂O₃ Catalyst, Ind. Eng. Chem. Res., vol. 27, no. 1, pp.51-57 (1988).
- 9- Sandler S. A., Chemical and Engineering Thermodynamics, 2nd edition, John Wiley and Sons, New York (1989).
- 10- Voorhies A., Deactivation of the reforming catalyst, Ind. Eng. Chem., Vol. 37, p. 318 (1945).
- 11- Froment G.F. and K.B. Bischoff, Chemical Reactor Analysis and Design, 2nd edition, John Wiley and Sons, New York (1990).

- 12- De Pauw R.P., and Froment G.F., Deactivation of a Platinum Reforming Catalyst in a Tubular Reactor, Chem. Eng. Sci., Vol. 30, pp. 789-801 (1974).
- 13- Ramage M.P., Graziani K.R., Schipper P.H., Krambeck F.J., B.C. Choi, KINPTR (Mobil's Reforming Model), A review of Mobil's Industrial Process Modeling Philosophy, Adv. in Chem. Eng., Vol. 13, pp. 193-266 (1987).
- 14- Turpin L.E., Modeling of commercial reformers, Chemical Industries, Vol. 61, p.437 (1994).
- 15- Varma A., "Packed bed reactor-an overview," Chemical Reactors, ed. Scott Fogler, ACS Symp. Series (1981).
- 16- Fogler S. H., Elements of Chemical Reaction Engineering, 3rd edition, Prentice-Hall, Inc., USA (2006).
- 17- Riazi M.R., and Daubert T.E., Simplify Property Predictions, Hydrocarbon Proc, 59(3), pp.115-120 (1980).
- 18- Press W.H., Teukolsky S.A., Vetterling W.J., Flannery B.P., Numerical Recipes in Fortran. The art of scientific computing, pp. 678-683, 2nd edition, Cambridge University Press, England (1992).
- 19- Marin G.B., and Froment G.F., Reforming of C₆ Hydrocarbons on a Pt-Al₂O₃ Catalyst, Chem. Eng. Sci, Vol. 37, No. 5, pp. 759-773 (1982)
- 20- Fazeli A., Fatemi S., Mahdavian M., Ghaee A., Mathematical Modeling of an Industrial Naphtha Reformer with Three Adiabatic Reactors in Series, Iran. J. Chem. Eng., Vol. 28, No.3, 2009.
- 21- Hou W., Suh H., Hu Y., Chu J., Modeling, Simulation and Optimization of a Whole Industrial Catalytic Naphtha Reforming Process on Aspen Plus Platform, Chinese J. Chem. Eng., 14(5) 584—591 (2006) .
- 22- Smith J.M., Chemical Engineering Kinetics, 3rd edition, McGraw-Hill International Edition, Singapore (1988).
- 23- Jamshid B. and Hamid R. K., A comparative Study for the Simulation and Optimization of Industrial Naphtha Reforming Reactors with Considering Pressure Drop on Catalyst, Petroleum & Coal 51(3), pp. 208-215 (2009).